Journal of The Electrochemical Society, **151** (7) B434-B439 (2004)
0013-4651/2004/151(7)/B434/6/$7.00 © The Electrochemical Society, Inc.

Microbiologically Induced Corrosion of 70Cu-30Ni Alloy in Anaerobic Seawater

Guangtuan Huang,[a] Kwong-Yu Chan,[b,*,z] and Herbert H. P. Fang[a]

[a]Department of Civil Engineering and [b]Department of Chemistry, The University of Hong Kong, Hong Kong Special Administrative Region, China

The corrosion of 70Cu-30Ni alloy induced by sulfate-reducing bacteria (SRB) in seawater was investigated by microscopic and electrochemical methods. Under anaerobic conditions, the SRB attached on the alloy surface formed blotchy biofilms, as observed by confocal laser scanning microscopy. Intergranular corrosion of the alloy occurred after immersion in SRB-containing seawater for 7 days, as observed by atomic force and scanning electron microscopy. Compared to the control experiment in the absence of SRB, a 330 mV shift of open-circuit potential resulted in the active direction and the polarization resistance decreased by a factor of 10. Electrochemical impedance spectroscopy data revealed that the impedance had remarkable capacitive characteristics. The response of the impedance was determined by two time constants for both the media with and without SRB. Analyses of concentrations of bacteria, metabolites, Cu, and Ni showed that the variation of concentrations of metabolites coincided with the growth of bacteria, and copper and nickel precipitated due to the production of metal sulfide. The effect of bacteria growth was the precipitation of cuprous sulfide to lower the potential of the anodic reaction and the reduction of hydrogen sulfide as the possible cathodic reaction.
 [DOI: 10.1149/1.1756153]

Manuscript submitted July 16, 2003; revised manuscript received January 29, 2004. Available electronically June 4, 2004.

The presence of microbes tends to enhance corrosion of metals either by the interactions of the excreted metabolites with the metal surface or by direct electrochemical reaction.[1] Microbiologically induced corrosion (MIC) by sulfate-reducing bacteria (SRB) in seawater has been extensively investigated.[2-11] Under normal circumstances, dissolved oxygen is the primary cathodic depolarizer in seawater. However, MIC may take place under anaerobic conditions when the seawater is polluted. SRB reduce sulfate in seawater to sulfide using pollutants as carbon and energy sources.[12] The biofilm formed on the metal surface maintains a radically different environment in terms of pH, dissolved oxygen, and other molecular/ionic species. The concentration gradients in the biofilm result in the formation of concentration cells on the metal surface.[13] Although the MIC of carbon steel and stainless steel have been widely studied, little is known about the MIC of SRB on copper and its alloys.[14-16]

Copper and its alloys are commonly used for structures and components exposed to seawater and other marine environments due to their corrosion resistance, machinability, and thermal and electrical conductivities. Cu-Ni alloys have good corrosion resistance in seawater because they form an oxide film comprising an outer layer of cupric hydroxy chloride, $Cu_2(OH)_3Cl$, overlaying a compact inner layer of cuprous oxide, Cu_2O. They also have good resistance to biofouling due to the toxicity of cupric ions. Copper-nickel alloys, such as 70Cu-30Ni and 90Cu-10Ni, are widely used in the air-conditioning systems of many coastal cities where seawater is used as the cooling medium.[17] However, MIC of Cu-Ni alloys was reported when bacteria were found entrapped between corrosion product layers containing extracellular polymers.[18]

In this study, MIC of 70Cu-30Ni alloy in anaerobic seawater containing SRB was investigated using electrochemical methods, such as open-circuit potential (OCP), polarization resistance, and electrochemical impedance spectroscopy (EIS). The seawater medium was analyzed for concentrations of bacteria, metabolites, Cu, and Ni. The attachment of bacteria on the surface was observed by confocal laser scanning microscopy (CLSM). The morphology of corrosion was examined by atomic force microscopy (AFM) and scanning electron microscopy (SEM).

Experimental

The bacterial sample was collected from a marine sediment in a complete-mixing reactor using modified Postgate's marine medium C at room temperature over 6 months. The medium contained 0.5 g KH_2PO_4, 1 g NH_4Cl, 0.06 g $CaCl_2 \cdot 6H_2O$, 0.06 g $MgSO_4 \cdot 7H_2O$, 6 mL sodium lactate (70%), 1 g yeast extract, 0.004 g $FeSO_4 \cdot 7H_2O$, and 0.3 g sodium citrate in each liter of natural seawater. The pH was adjusted to 7.2 ± 0.1 using 1 M NaOH solution. The medium was autoclaved at 121°C for 15 min and then purged with pure nitrogen for 1 h to remove dissolved oxygen. The bacteria sample was inoculated into the medium at room temperature for 3 days and then stored in the refrigerator. Before every experiment, the bacteria sample was activated in the same medium at room temperature for 3 days and inoculated into the medium.

Cylindrical specimens 12.7 mm diam, 3 mm thick, were cut from 70Cu-30Ni alloy rod supplied by Goodfellow Cambridge Limited. The exact chemical composition is 70.24% Cu, 29.20% Ni, 0.45% Fe, and 0.02% Mn. Cylindrical specimens were embedded in an epoxy cold mounting resin with electrical contact achieved by welding a copper wire into the base of the metal sample. Prior to each experiment, the exposed surfaces were sequentially abraded by using 400–1500 meshes silicon carbide emery papers, and polished to a smooth surface finish by using 0.3 μm alumina paste, then rinsed with deionized (DI) water, degreased with acetone, sterilized by immersion in ethanol, and dried by purging with pure nitrogen.

The OCP was recorded using an Autolab/PGTSTAT30 potentiostat. Measurement of the polarization resistance was performed by potentiodynamically polarizing from −20 mV to +20 mV *vs.* OCP at a sweep rate of 1 mV/s. This range was larger than the usual range of −10 mV to +10 mV to accommodate possible drifts of the

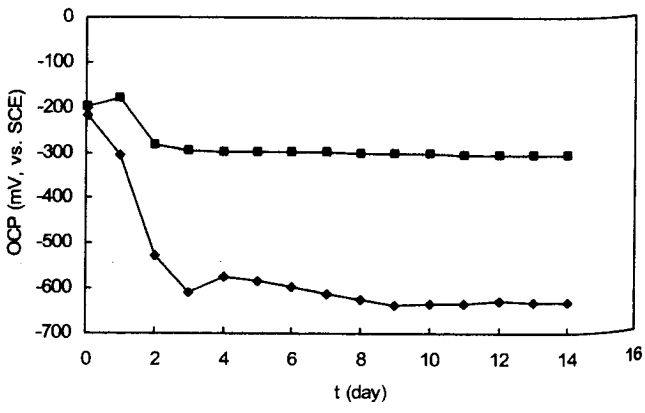

Figure 1. OCP *vs.* time for 70Cu-30Ni alloy in modified Postgate's marine medium C, not inoculated (squares) and inoculated (diamonds) with SRB.

* Electrochemical Society Active Member.
z E-mail: hrsccky@hku.hk

Table I. Polarization resistance and Tafel slope *vs.* time for 70Cu-30Ni alloy in modified Postgate's marine medium C not inoculated and inoculated with SRB.

	Not inoculated with SRB			Inoculated with SRB		
t (days)	b_c (mV/dec)	b_a (mV/dec)	R_p (kohm cm^2)	b_c (mV/dec)	b_a (mV/dec)	R_p (kohm cm^2)
0	66	45	3.1	38	27	7.4
2	45	47	178.4	21	40	135.4
4	11	44	184.8	15	28	107.5
6	19	42	195.0	12	31	44.8
8	21	32	196.5	13	27	30.3
10	15	41	229.8	8	39	26.5
12	27	39	228.6	12	31	23.4
14	22	38	260.9	6	25	21.9

OCP. EIS was conducted by using an Autolab/PGTSTAT30 and FRA2 module in combination with frequency response analysis software. The exposed area of the working electrode was 1.266 cm^2. A high-density graphite rod was used as the auxiliary electrode, and a saturated calomel electrode (SCE) was used as the reference electrode. All the potentials were measured with respect to SCE. A sinusoid wave of ±10 mV was applied at OCP in the frequency range from 100 kHz to 0.001 Hz.

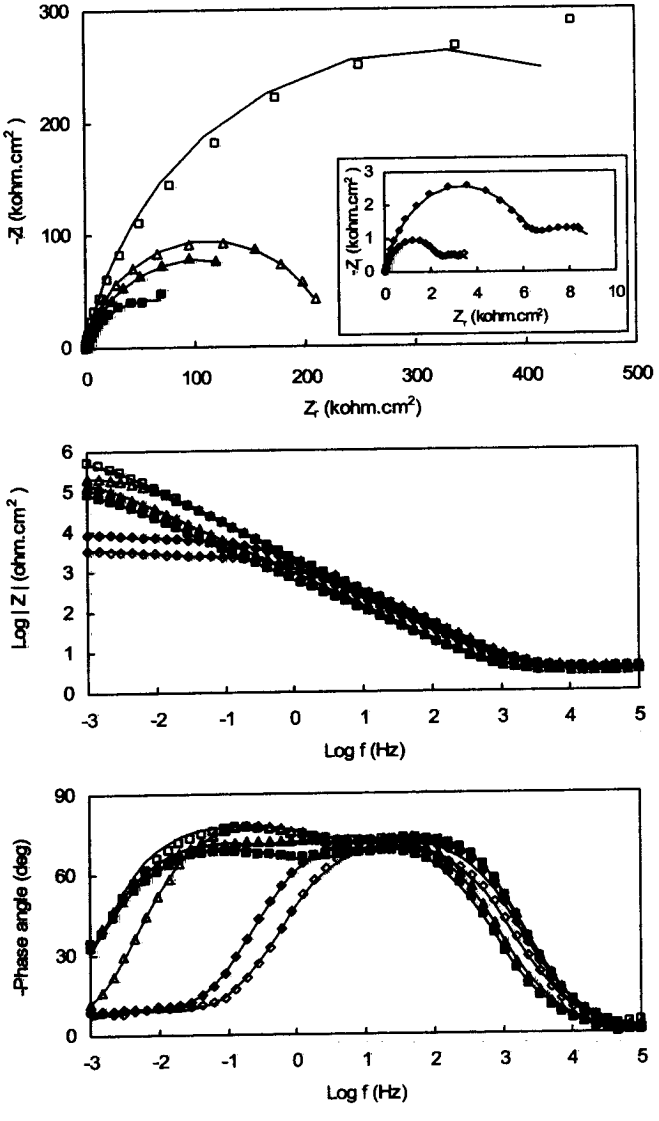

Figure 2. EIS of 70Cu-30Ni alloy in modified Postgate's marine medium C not inoculated with SRB for 2 h (open diamonds), 7 days (open triangles), and 14 days (open squares) and inoculated with SRB for 2 h (solid diamonds), 7 days (solid triangles), and 14 days (solid squares). Solid lines represent the fitted results based on the equivalent circuit.

The bacterial growth was monitored by fluorescence microscopy (Nikkon Eclipse E600). To a volume 100 μL culture solution was added 100 μL of 100 μg/L DAPI. 100. This solution was stained for 10 min, vortexed for 1 min, and filtered through a 0.4 μm polycarbonate membrane (black) supplied by Osmonics Inc. The membrane was placed under fluorescence microscopy to count the number of bacteria. Sulfide was measured by the mixed diamine reagent colorimetric method.[19] The concentrations of acetic acid and isobutyric acid were measured by gas chromatography. The amounts of dissolved copper and nickel were determined by atomic absorption spectroscopy.

The specimens exposed in the same electrochemical cell were observed by CLSM, AFM, and SEM. Specimens for CLSM were blotted and covered with 200 μL SYTO9 to stain the biofilm at room temperature for 20 min. After staining, the phosphate buffer solution was carefully added to the specimens and drawn off with filter paper to remove the unbound probes. Images were acquired with a Zeiss LSM 5 Pascal laser scanning confocal microscope (Zeiss, Jena, Germany). Specimens for AFM were directly rinsed through seawater/DI water washes to deionized water and dried by purging with pure nitrogen. Specimens were examined using a Nanoscope IIIA atomic force microscope (Digital Instruments, Santa Barbara, CA) in contact mode with standard etched silicon nitride probes. Specimens for SEM were fixed in 4% glutaraldehyde in 0.2 μm filtered seawater, rinsed through seawater/DI water washes to DI water, and dehydrated through ethanol/DI water from 50/50 to 100% ethanol. Specimens were observed by using SEM (Steroscan 360, Cambridge, UK).

Results and Discussion

OCP.—The monitoring of OCP can provide some information on the evolution of the corrosion process. Sudden changes of the potential in the active direction are useful for detecting the initiation of accelerated attack due to the growth of bacteria. In Fig. 1, the OCP is shifted to the active direction with respect to the absence of SRB during the growth of SRB. The OCP rapidly decreases to −630 mV for the medium inoculated with SBR and −300 mV for the control experiment not inoculated with SRB. The OCP increases slightly for the medium inoculated with SRB in the first day. Shalaby *et al.*[15] explained that the shift of the OCP to the active direction was attributed to the enhancement of the anodic process in terms of the mixed potential theory. In the present work, both the formation of a protective film and the growth of SRB have an effect on the anodic and cathodic processes. In the absence of SRB, the protective film retards the anodic dissolution of copper alloy further. In the presence of SRB, the growth of SRB promotes the anodic process, and the surface film is poorly protective due to the formation of Cu_2S. Therefore, the OCP is shifted to a more active direction compared with a medium where the SRB are absent.

Polarization resistance.—Polarization resistance is defined as the

Table II. Fitting parameters of EIS of 70Cu-30Ni alloy in modified Postgate's marine medium C not inoculated with SRB.

t (days)	R_s (ohm cm^2)	R_1 (ohm cm^2)	Y_{01} (F/cm^2)	n_1	R_2 (kohm cm^2)	Y_{02} (F/cm^2)	n_2
0	3.7	2396.0	2.56×10^{-5}	0.83	1.6	6.90×10^{-4}	0.65
1	3.2	5630.0	4.83×10^{-5}	0.88	9.5	1.09×10^{-5}	0.58
7	3.9	166.7	4.36×10^{-5}	0.85	222.7	3.24×10^{-5}	0.90
10	3.6	139.9	5.99×10^{-5}	0.85	429.0	3.06×10^{-5}	0.89
14	3.5	125.4	7.59×10^{-5}	0.85	629.0	2.96×10^{-5}	0.89

derivative of the potential with respect to the current at the free corrosion potential (E_{corr}). This is determined as the slope of a polarization curve at E_{corr}, where the current is equal to zero.[13] Polarization resistance qualitatively reflects the corrosion resistance of metals in the medium. Table I presents the data of polarization resistance and Tafel slope for 70Cu-30Ni alloy in the modified Postgate's marine medium C not inoculated and inoculated with SRB. It shows that the polarization resistance increases with exposure time during the first 2 days whether or not the sample is inoculated with SRB. In the presence of SRB, the maximum polarization resistance is smaller than that in the absence of SRB. After an exposure of 10 days, the polarization resistance decreases to about one-tenth of that of the control. This suggests that the growth of SRB accelerates the corrosion rate of 70Cu-30Ni alloy in anaerobic seawater by a factor of 10.

Generally, the Tafel slope reflects the kinetics of the corrosion process. It was reported that the average values of the anodic Tafel slope (b_a) of copper alloys in artificial and natural seawater were approximately 60 mV/dec in the presence of oxygen.[20] Kato and Pickering[21] suggested that a Tafel slope of 60 mV/dec can be attributed to a one-electron transfer reaction with diffusion of a reactant or product in the aqueous phase being the rate-determining step. For copper alloys exposed in seawater, transport of Cl^- to or transport of $CuCl_2^-$ from the surface is the rate-determining step. In the present work, the average value of b_a is approximately 40 mV/dec in the absence of SRB and about 30 mV/dec in the presence of SRB. The smaller values indicate that the transfer of electrons is easier. The anodic process is enhanced due to the growth of SRB. In both cases, the values of cathodic Tafel slope (b_c) are scattered with respect to different days of corrosion. Except for one day, the cathodic Tafel slopes in the solution inoculated with SRB are generally lower than those in the solution not inoculated with SRB. It is unclear whether the enhanced cathode kinetics is caused directly by the growth process of SRB or indirectly by the produced hydrogen sulfide and acidic metabolites such as acetic acid and isobutyric acid. It is suggested that the presence of hydrogen sulfide and acidic metabolites have a significant effect on the cathodic processes.

EIS.—EIS is a powerful, nondestructive electrochemical technique for characterizing electrochemical reactions at the metal/biofilm interface and the formation of corrosion products and biofilm in MIC. Figure 2 illustrates EIS of 70Cu-30Ni alloy in the modified Postgate's marine medium C inoculated and not inoculated with SRB for 2 h, 7 days, and 14 days. The frequency dependence of the phase angle shows that the impedance has remarkable capacitive characteristics, and the response of the impedance is determined by two time constants. The impedance remarkably increases across a large frequency domain with exposure time in the absence of SRB. This increase is associated with an increase of the phase angle peak at low frequency and its shift to lower frequencies. This suggests that the protective film is gradually formed and retards the progress of corrosion. The total impedance increases first and then decreases with exposure time in the presence of SRB. But the impedance generally decreases with exposure time at high frequency. These changes reflect the formation and damage of the protective film and the acceleration of corrosion. This behavior is similar to that of 70Cu-30Zn alloy in API RP-38 medium.[14] Moreover, during the first 2 h, the impedance in the presence of SRB is larger than that in the absence of SRB. This may be due to the effect of sulfide added with the inoculum.

Considering the effects of the surface film and electrochemical reactions, the following equivalent model circuit (Scheme 1) is used to fit the EIS data

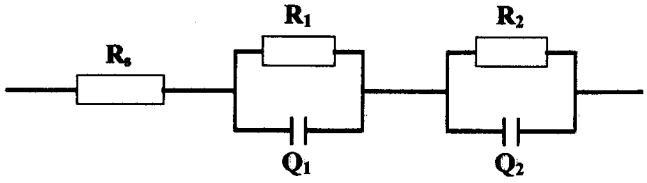

Scheme I.

Here, R_1 is the electric resistance of charge transfer, R_2 is the electric resistance of the surface film, Q_1 is the constant-phase element (CPE) of the electric double layer, and Q_2 is the CPE of the surface film.
The impedance of the CPE, Q, is expressed as

$$Z = \frac{1}{Y_0}\omega^{-n}\left[\cos\frac{n\pi}{2} - j\sin\frac{n\pi}{2}\right] \quad (0 < n < 1) \qquad [1]$$

Tables II and III give the fitting parameters of EIS of 70Cu-30Ni alloy in modified Postgate's marine medium C not inoculated and inoculated with SRB. R_s denotes the resistance of the solution, which is basically identical for the medium inoculated or not inoculated with SRB. n is the dispersion parameter, which is related to the roughness of the electrode and the conductivity of the solution. Generally the rougher the surface, the smaller the conductivity and the smaller the value of n. Y_0 denotes the parameter related to the capacitance. In Tables II and III, the data of R_1, Y_{01}, Y_{02}, n_1, and n_2 do not have a clear trend, which is related to the complexity of the impedance spectra caused by the formation of the corrosion product

Table III. Fitting parameters of EIS of 70Cu-30Ni alloy in modified Postgate's marine medium C inoculated with SRB.

t (days)	R_s (ohm cm^2)	R_1 (ohm cm^2)	Y_{01} (F/cm^2)	n_1	R_2 (kohm cm^2)	Y_{02} (F/cm^2)	n_2
0	3.3	3230.0	2.65×10^{-3}	0.79	6.5	2.10×10^{-5}	0.84
1	3.2	87.1	1.47×10^{-4}	0.85	172.3	2.41×10^{-5}	0.88
7	3.2	215.7	7.04×10^{-4}	0.88	203.9	4.95×10^{-5}	0.83
10	3.3	46.2	9.80×10^{-4}	0.96	128.0	4.87×10^{-5}	0.81
14	3.3	100.0	3.78×10^{-4}	0.88	117.4	6.12×10^{-5}	0.80

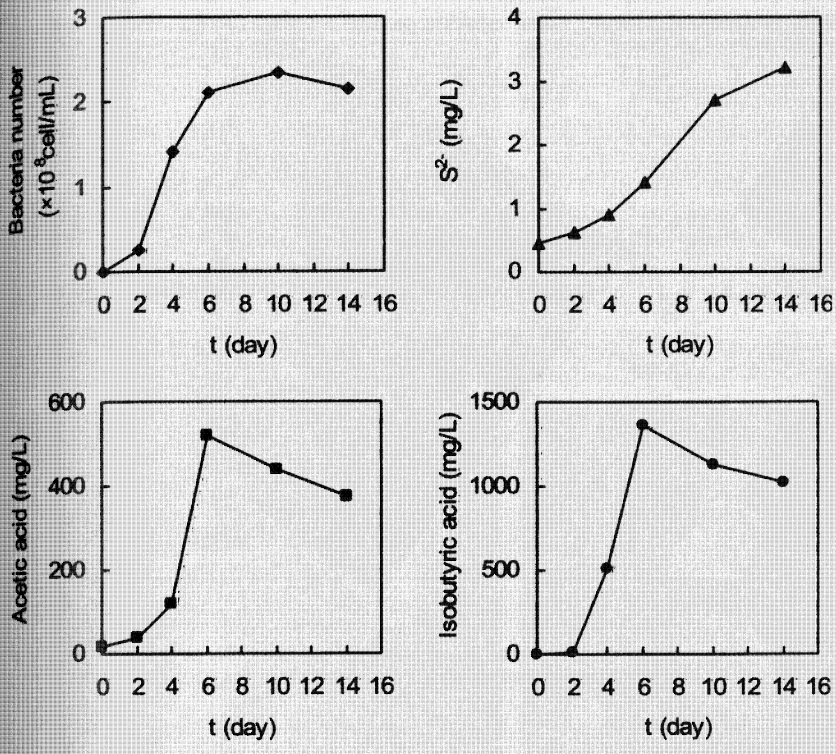

Figure 3. Variation of bacteria number, sulfide, acetic acid, and isobutyric acid with cultivation time for 70Cu-30Ni alloy in modified Postgate's marine medium C inoculated with SRB.

layer and the biofilm. The values of R_2 initially increase and then decrease with exposure time for the absence of SRB. This trend is consistent with that of polarization resistance.

Analysis of culture medium.—Figure 3 illustrates the variation of bacteria number, sulfide, acetic acid, and isobutyric acid with cultivation time for 70Cu-30Ni alloy in modified Postgate's marine medium C inoculated with SRB. The bacteria number rapidly increases during the first 6 days and then does not change after 6 days. This is the growth curve of SRB in this medium. The concentration of sulfide gradually increases with cultivation time. The concentrations of acetic acid and isobutyric acid, which are metabolic products of SRB, increase rapidly during the first 6 days and then slightly decrease. This trend is similar to the growth curve. In comparison with the variation of polarization resistance, it seems that the growth process of bacteria coincides with the formation and damage of the protective film and the acceleration of corrosion. The final decrease of metabolic products of SRB with time could be due to impure inoculum of SRB. Other bacteria may be present in the medium, such as methane-producing bacteria, which can utilize acidic metabolites as substrates.

Figure 4 illustrates the variation of the concentrations of copper and nickel with exposure time for 70Cu-30Ni alloy in modified Postgate's marine medium C not inoculated and inoculated with SRB. In the absence of SRB, the concentrations of copper and nickel are an order of magnitude higher than those in the presence of SRB. It suggests that copper and nickel precipitate due to the production of metal sulfide. From this, it is supposed that the production of hydrogen and the precipitation of metal sulfide may have an effect on the corrosion process of 70Cu-30Ni alloy in the medium. The concentration of copper is lower than nickel in the presence of SRB, suggesting the easier precipitation of cuprous sulfide.

CLSM.—Figure 5 illustrates the CLSM images of 70Cu-30Ni alloy in modified Postgate's marine medium C inoculated with SRB for 7 days and 14 days. It is seen that SRB attach on the surface of the 70Cu-30Ni alloy. With increasing exposure time, the coverage area of bacteria on the surface increases, but the bacteria do not form a continuous biofilm as in the case of mild steel.

AFM.—Figure 6 illustrates the three-dimensional (3D) AFM images of 70Cu-30Ni alloy in modified Postgate's marine medium C, not inoculated and inoculated with SRB for 2 h, 7 days, and 14 days. In the absence of SRB, the protective film thickens with exposure time, and there are no apparent pits on the surface. In the presence

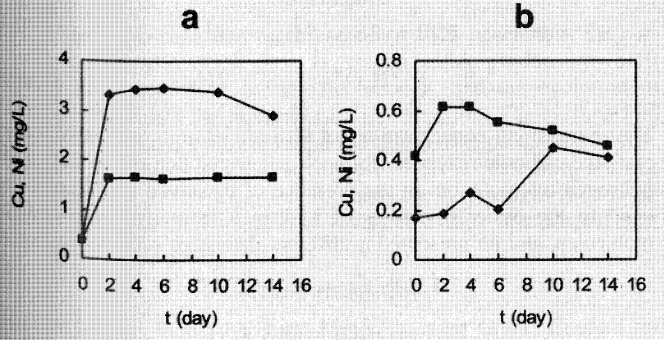

Figure 4. Variation of the concentrations of copper (diamonds) and nickel (squares) with exposure time for 70Cu-30Ni alloy in modified Postgate's marine medium C, (a) not inoculated and (b) inoculated with SRB.

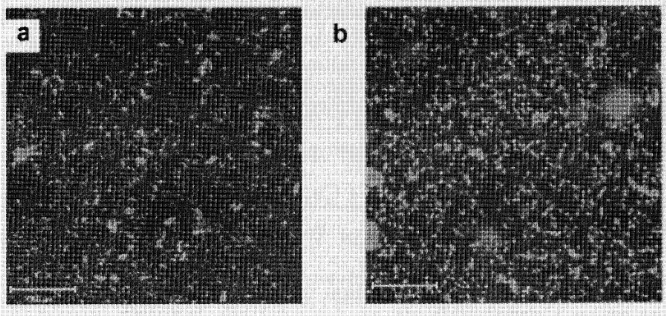

Figure 5. CLSM images of 70Cu-30Ni alloy in modified Postgate's marine medium C, inoculated with SRB for (a) 7 days and (b) 14 days. Both scale bars are 50 μm.

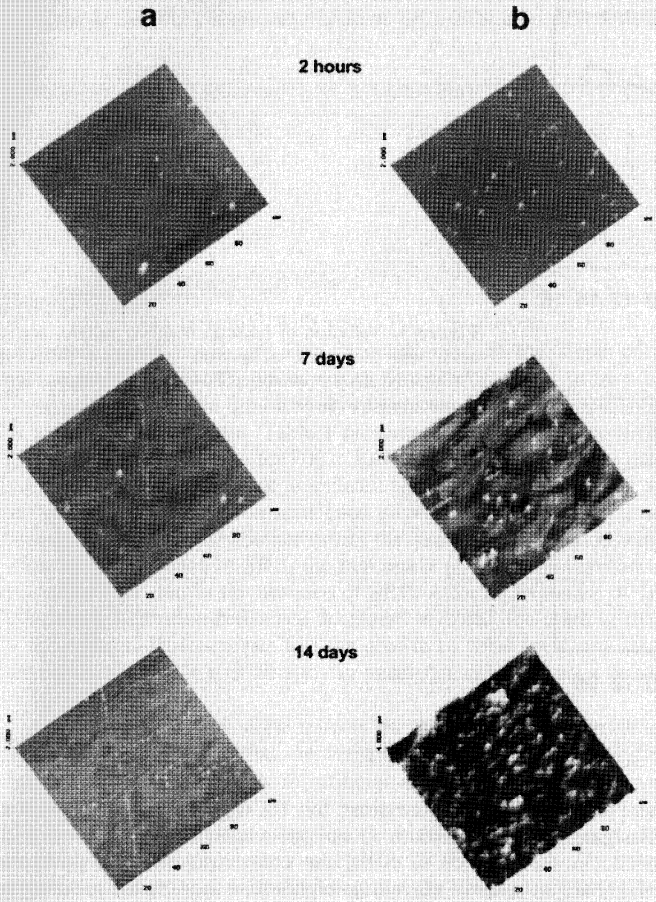

Figure 6. 3D AFM images of 70Cu-30Ni alloy in modified Postgate's marine medium C, (a) not inoculated and (b) inoculated with SRB for 2 h, 7 days, and 14 days.

of SRB, crevices can be observed on the surface of the specimen after 7 days. An enlarged image of this 7 day sample with SRB is shown in Fig. 7. These crevices seem to emerge along the grain boundaries of the metal. It reveals that intergranular corrosion takes place in this condition. The grain boundary can be seen only when it is preferentially dissolved in the medium. With increasing exposure time, crevices are enlarged and grooves are formed. It was reported that intergranular corrosion was observed on the surface of 70Cu-30Ni alloy after 1 month exposure to natural seawater.[16]

SEM.—Figure 8 illustrates the SEM images of 70Cu-30Ni alloy in modified Postgate's marine medium C inoculated with SRB for 14 days. Cracking-off of corrosion products and pits are developed on the surface of specimens. It is suggested that the surface film is fragile and poorly protective.

The acceleration of corrosion and occurrence of intergranular corrosion in the presence of SRB must be considered from electrochemical reactions of copper alloys in seawater. Based on the potential-pH diagram for copper in sulfide-free seawater,[22] the corrosion products can be CuCl, $CuCl_2^-$, and Cu_2O. One of the possible anodic reaction of copper alloys is

$$2Cu + 2OH^- \rightarrow Cu_2O + H_2O + 2e$$
$$E_o = -0.358 \text{ V } (vs. \text{ SCE}) \quad [2]$$

The other possible anodic reaction is[23]

$$Cu + Cl^- \rightarrow CuCl + e \quad E_o = 0.137 \text{ V } (vs. \text{ SCE}) \quad [3]$$

followed by the formation of cuprous complex[24]

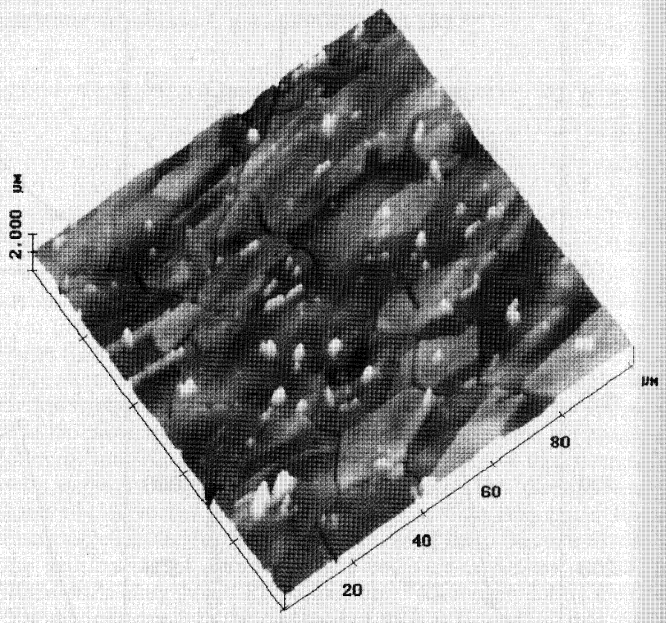

Figure 7. Enlarged 3D AFM image of 70Cu-30Ni alloy in modified Postgate's marine medium C inoculated with SRB for 7 days.

$$CuCl + Cl^- \rightarrow CuCl_2^- \quad [4]$$

In deaerated seawater, the cathodic reaction is

$$2H^+ + 2e \rightarrow H_2 \quad E_o = -0.244 \text{ V } (vs. \text{ SCE}) \quad [5]$$

Based on the standard electrode potentials of the anodic and cathodic reactions, clearly, the anodic reaction of copper to cuprous oxide proceeds more easily.

In the presence of sulfide, the most possible corrosion product is cuprous sulfide based on the potential-pH diagram for copper in sulfide-polluted seawater.[22] The most possible anodic reaction is

$$2Cu + S^{2-} \rightarrow Cu_2S + 2e \quad E_o = -0.540 \text{ V} \quad [6]$$

In addition, Eiselstein *et al.*[25] proposed that sulfide ions reacted with cuprous ions to form cuprous sulfide, and the decrease in the concentration of cuprous ion caused the anodic reaction of copper to cuprous ion to be shifted to the lower potentials.

A possible cathodic reaction is the evolution of hydrogen. However, Kaesche[26] suggested that the discharge of hydrogen ions from H_2S molecules was energetically more advantageous than the discharge of hydronium ions (H_3O^+), due to the lower dissociation energy of the HS—H bond compared to the HO—H bond. He proposed that the processes of the reduction and regeneration of H_2S molecules were as follows

$$H_2S + 2e \rightarrow 2H_{ads} + S^{2-} \quad [7]$$

$$S^{2-} + 2H_3O^+ \rightleftharpoons H_2S + 2H_2O \quad [8]$$

Therefore, small concentrations of H_2S are enough to greatly accelerate the cathodic reaction. Bolmer[27] suggested that the reduction of hydrogen overpotential in the presence of dissolved sulfide was related to the easier discharge of hydrogen from hydrogen sulfide molecules, and he presented a different discharge scheme

$$2H_2S + 2e \rightarrow H_2 + 2HS^- \quad [9]$$

$$HS^- + H_3O^+ \rightleftharpoons H_2S + H_2O \quad [10]$$

As mentioned, hydrogen sulfide plays an important role in the corrosion process of copper alloys in sulfide-polluted seawater. In the

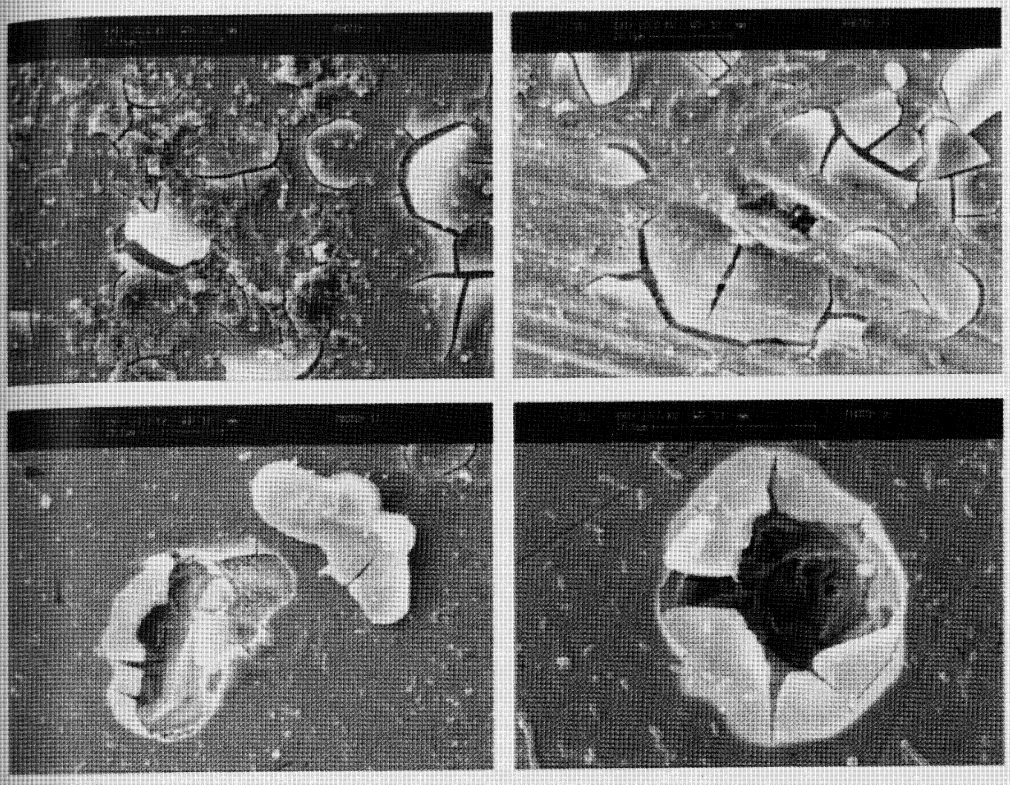

Figure 8. SEM images of 70Cu-30Ni alloy in modified Postgate's marine medium C inoculated with SRB for 14 days.

present work, the effect of SRB is that the biofilm attached on the surface creates local electrochemical cells, hydrogen sulfide produced by SRB reacts with the cuprous ions from anodic reaction or participates in the anodic reaction directly to form cuprous sulfide, and the reduction of hydrogen sulfide becomes the possible cathodic reaction as a substitute for the evolution of hydrogen. Because of the formation of cuprous sulfide, the surface film becomes fragile and poorly protective. The production of organic acids lowers the pH of the medium and accelerates the cathodic reaction. The precipitation of cuprous sulfide lowers the potential of the anodic reaction and enhances the anodic process. Therefore, the process of corrosion accelerates in the presence of SRB. The cracking-off of the surface film, the emergence of the pits, and the heterogenicity of the local environment produced by the biofilm bring about intergranular corrosion. To investigate the discussed corrosion mechanism, analyses of the compositions of the sample surfaces, such as energy dispersive x-ray analysis should be performed. Such elemental analyses can provide evidence for possible corrosion products formed on the surface and support certain reaction pathways. These surface composition analyses for samples with different immersion times are highly desirable in future investigations.

Conclusions

In anaerobic seawater, the presence of SRB accelerates the corrosion rate of 70Cu-30Ni alloy. Hydrogen sulfide produced by SRB lowers the potential of the anodic reaction, and the evolution of hydrogen becomes the possible cathodic reaction. The surface film is poorly protective because of the formation of cuprous sulfide. The attachment of biofilm, the cracking-off of the surface film, and the heterogenicity of the local environment are responsible for the attack of intergranular corrosion of 70Cu-30Ni alloy in anaerobic seawater containing SRB.

Acknowledgment

The authors thank the Hong Kong Research Grants Council for the financial support (HKU 7004/00E) of this study.

The University of Hong Kong assisted in meeting the publication costs of this article.

References

1. J. Telegdi, Zs. Keresztes, G. Pálinkás, E. Kálmán, and W. Sand, *Appl. Phys. A: Mater. Sci. Process.*, **66**, S639 (1998).
2. K. Y. Chan, L. C. Xu, and H. H. P. Fang, *Environ. Sci. Technol.*, **36**, 1720 (2002).
3. H. Liu, L. Xu, and J. Zeng, *Br. Corros. J., London*, **35**, 131 (2000).
4. H. A. Videla, *Biofouling*, **15**, 37 (2000).
5. L. C. Xu, H. H. P. Fang, and K. Y. Chan, *J. Electrochem. Soc.*, **146**, 4455 (1999).
6. H. Tributsch, J. A. Rojas-Chapana, and C. C. Bartels, *Corrosion (Houston)*, **54**, 216 (1998).
7. A. Neville and T. Hodgkiss, *Br. Corros. J., London*, **35**, 60 (2000).
8. R. P. George, P. Muraleedharan, N. Parvathavarthini, J. B. Gnanamoorthy, T. S. Rao, and K. V. K. Nair, *T. Indian I. Metals*, **51**, 331 (1998).
9. J. E. G. Gonzalez, F. J. H. Santana, and J. C. Mirza-Rosca, *Corros. Sci.*, **40**, 2141 (1998).
10. P. Angell, J. S. Luo, and D. C. White, *Corros. Sci.*, **37**, 1085 (1995).
11. H. Amaya and H. Miyuki, *J. Jpn. Inst. Met.*, **58**, 775 (1994).
12. J. Mathiyarasu, N. Palaniswamy, and V. S. Muralidharan, *Corros. Rev.*, **18**, 65 (2000).
13. B. Little, P. A. Wagner, and F. Mansfeld, *Microbiologically Influenced Corrosion*, B. C. Syrett, Series Editor, p. 4, NACE International, Houston (1997).
14. J. Liu, J. Zheng, and L. Xu, *Mater. Corros.*, **52**, 833 (2001).
15. H. M. Shalaby, A. A. Hasan, and F. Al-Sabti, *Br. Corros. J., London*, **34**, 292 (1999).
16. F. Mansfeld and B. Little, *Electrochim. Acta*, **37**, 2291 (1992).
17. S. M. Sayed, E. A. Ashour, and G. I. Youssef, *Mater. Chem. Phys.*, **78**, 825 (2003).
18. G. Blunn, in *Biodeterioration 6: Biological Fouling of Copper and Copper Alloys*, S. Barry, D. R. Houghton, G. C. Llewellyn, and C. E. O'Rear, Editors, p. 567, CAB International, Slough (1986).
19. EPA 821/R-91-100, *Analytical Method for Determination of Acid Volatile Sulfide in Sediment*, Office of Science and Technology Health and Ecological Criteria Division, Washington, DC (1991).
20. F. Mansfeld, G. Liu, H. Xiao, C. H. Tsai, and B. Little, *Corros. Sci.*, **36**, 2063 (1994).
21. C. Kato and H. Pickering, *J. Electrochem. Soc.*, **131**, 1219 (1984).
22. D. D. Macdonald, B. C. Syrett, and S. S. Wing, *Corrosion (Houston)*, **35**, 367 (1979).
23. W. D. Bjorndahl and K. Nobe, *Corrosion (Houston)*, **40**, 82 (1984).
24. G. Faita, G. Fiori, and D. Salvador, *Corros. Sci.*, **15**, 383 (1975).
25. L. E. Eiselstein, B. C. Syrett, S. S. Wing, and R. D. Caligiuri, *Corros. Sci.*, **23**, 223 (1983).
26. H. Kaesche, *Werkst. Korros.*, **21**, 185 (1970).
27. P. Bolmer, *Corrosion (Houston)* **21**, 69 (1965).